



OPEN

Ferroelectric Polarization in
Nanocrystalline Hydroxyapatite Thin
Films on SiliconSUBJECT AREAS:
BIOMINERALIZATION
BIOPHYSICAL METHODS
BIOENERGETICS
BIOMEDICAL MATERIALSS. B. Lang¹, S. A. M. Tofail^{2,8}, A. L. Kholkin³, M. Wojtas^{3,7}, M. Gregor⁴, A. A. Gandhi^{2,8}, Y. Wang⁵,
S. Bauer⁶, M. Krause⁶ & A. Plecenik⁴Received
5 April 2013Accepted
2 July 2013Published
25 July 2013Correspondence and
requests for materials
should be addressed to
S.B.L. (lang@bgu.ac.il)
or S.A.M.T. (tofail.
syed@ul.ie)

¹Ben-Gurion University of the Negev, Beer Sheva, Israel, ²Department of Physics and Energy, University of Limerick, Limerick, Ireland, ³University of Aveiro, Aveiro, Portugal, ⁴Comenius University, Bratislava, Slovakia, ⁵Hong Kong Polytechnic University, Hong Kong, ⁶Johannes Kepler University, Linz, Austria, ⁷University of Wroclaw, Wroclaw, Poland, ⁸Energy, Materials and Surface Science Institute, University of Limerick, Limerick, Ireland.

Hydroxyapatite nanocrystals in natural form are a major component of bone- a known piezoelectric material. Synthetic hydroxyapatite is widely used in bone grafts and prosthetic pyroelectric coatings as it binds strongly with natural bone. Nanocrystalline synthetic hydroxyapatite films have recently been found to exhibit strong piezoelectricity and pyroelectricity. While a spontaneous polarization in hydroxyapatite has been predicted since 2005, the reversibility of this polarization (i.e. ferroelectricity) requires experimental evidence. Here we use piezoresponse force microscopy to demonstrate that nanocrystalline hydroxyapatite indeed exhibits ferroelectricity: a reversal of polarization under an electrical field. This finding will strengthen investigations on the role of electrical polarization in biomineralization and bone-density related diseases. As hydroxyapatite is one of the most common biocompatible materials, our findings will also stimulate systematic exploration of lead and rare-metal free ferroelectric devices for potential applications in areas as diverse as *in vivo* and *ex vivo* energy harvesting, biosensing and electronics.

Hydroxyapatite nanocrystals are one of the fundamental building blocks of bone and the primary determinant of bone density and mechanical stability. Hydroxyapatite concretions are even found in the pineal gland of the brain¹. Synthetic hydroxyapatite is widely used in bone grafts and prosthetic coatings as it binds strongly with natural bone – a critical requirement especially when the host bone-density is low due to age or diseases (e.g. osteoporosis). Electrical polarization, on the other hand, is believed to be significant in biomineralisation in living animals². Polarized hydroxyapatite has been found to stimulate the growth of bone-like apatite both *in vitro*³ and *in vivo*⁴. Thin Films of nanocrystalline hydroxyapatite exhibit strong piezoelectricity and pyroelectricity, the magnitude of which are of the order shown by piezoelectric material zinc oxide (ZnO) and ferroelectric material polyvinylidene fluoride (PVDF), respectively. Here we show that, unlike ZnO and similar to PVDF, nanocrystalline hydroxyapatite films show reversible spontaneous polarization of a ferroelectric nature. The remnant polarization is about a quarter of that measured for a lead-zirconate-titanate (PZT) film measured under similar conditions.

While ferroelectricity in soft tissues such as aortic wall and components has been claimed for a long time^{5–8}, hard tissues (e.g. lamellar bone⁹) and its constituents (e.g. collagen¹⁰) typically exhibited anti-ferroelectric order. In contrast, we find that hydroxyapatite reveals a ferroelectric order, which is stabilized due to its nanoscale dimension¹¹. This finding will stimulate new understanding of the mechanism of biomineralisation and the formation of the characteristic hierarchical structure of bone. Reversible spontaneous polarization in hydroxyapatite will also open up a number of novel technical applications such as in electronics, microelectromechanical systems (MEMS), *in vivo* energy harvesting and biosensors.

Ferroelectricity is a property of reversibility of spontaneous polarization (P_s) by the application of an electric field. Such property is shown by a small subset of pyroelectric materials that belongs to one of the ten crystal classes that possess a spontaneous polarization and no center of symmetry. A pyroelectric material, typically termed as a polar material due to the presence of spontaneous polarisation, generates electrical charge proportional to the rate of change of temperature. A pyroelectric material also shows piezoelectricity- the ability to generate electrical charge proportional to the applied strain and vice versa. It is a property of crystals that possess no center of symmetry. There are 21 crystal classes that possess no center of symmetry, 20 of which are piezoelectric.



A piezoelectric effect in bone was first observed by Fukada and Yasuda in 1957¹². Pyroelectricity of bone has also been reported¹³. Until very recently, the effect was believed to be due to the collagen component of bone because hydroxyapatite was considered to be centrosymmetric¹⁴. In 2005 Haverly *et al.* proposed two polar symmetries for hydroxyapatite: a monoclinic $P2_1$ and a hexagonal $P6_3$, which do not possess any centre of symmetry¹⁵. These polar, non-centrosymmetric structures originated from a ferroelectric ordering of the hydroxyl ions (OH) along the crystallographic c axis ([001] direction) (as shown in Figure 1). In fact, an antiferroelectric to ferroelectric transition was deemed possible¹⁶ although no experimental proof of ferroelectricity in hydroxyapatite has so far been reported.

The small energy difference between these polar symmetries and the non polar centro-symmetric structure (commonly denoted by a $P2_1/b$ symmetry) means that smaller size in hydroxyapatite crystals may lead to the stability of these polar structures due to the availability of large amounts of surface energy. Indeed, an X-ray Diffraction (XRD) experiment has revealed that nanocrystalline hydroxyapatite (SRM2910)¹⁷ is predominantly polar (77%). A pyroelectric surface charge in electrically poled hydroxyapatite ceramics¹⁸ and a very weak shear piezoelectric effect in unpoled hydroxyapatite ceramic¹⁹ have been observed. The manifestation of polar effects was however weak due to the averaging effect and larger grain sizes in hydroxyapatite ceramics ($\sim 1\text{--}5\ \mu\text{m}$). This has been overcome in nanocrystalline thin films of hydroxyapatite deposited on Si. In 2011, Lang *et al.* reported the first measurements of a piezoelectric

coefficient in hydroxyapatite thin films ($16\ \text{pC N}^{-1}$) and a pyroelectric coefficient ($12\ \mu\text{C m}^{-2}\ \text{K}^{-1}$)²⁰, which are similar to the values for PVDF²¹ and ZnO²² thin films.

Recently, Chiatti *et al.*¹¹ have investigated the stability of the OH-terminated (001) surface of hydroxyapatite that essentially gives hydroxyapatite its characteristic needle shape morphology due to the growth of hydroxyapatite along its crystallographic c -axis. They found that hydroxyapatite (001) surface can be stable with a ferroelectric ordering of OH at a nanometric scale up to the limit of their measurements (43 nm thickness of a slab). In essence, they claimed that the hydroxyapatite (001) surface can be considered as made of one dimensional (1-D) ferroelectric wires (i.e. the OH columns within the channel formed by the so called Ca-triangles) embedded in a dielectric medium consisting of Ca ions and PO_4 ions that can counterpolarize the internal field. The implication of this finding is that ferroelectricity may be more probable in nanocrystalline hydroxyapatite. Our work confirms this expectation.

Results

We carried out investigations in order to prove ferroelectric behavior in nanocrystalline hydroxyapatite by Piezoresponse Force Microscopy (PFM), which has recently shown to be a very sensitive measurement technique for piezo- and ferroelectricity measurements in nanostructural and biological systems^{23,24}. It has been used for the detection of biopiezo- and ferroelectricity in peptide nanotubes^{25,26} and amino acid glycine²⁷ where both domain assemblies and polarization switching could be observed on the scale of a few nm.

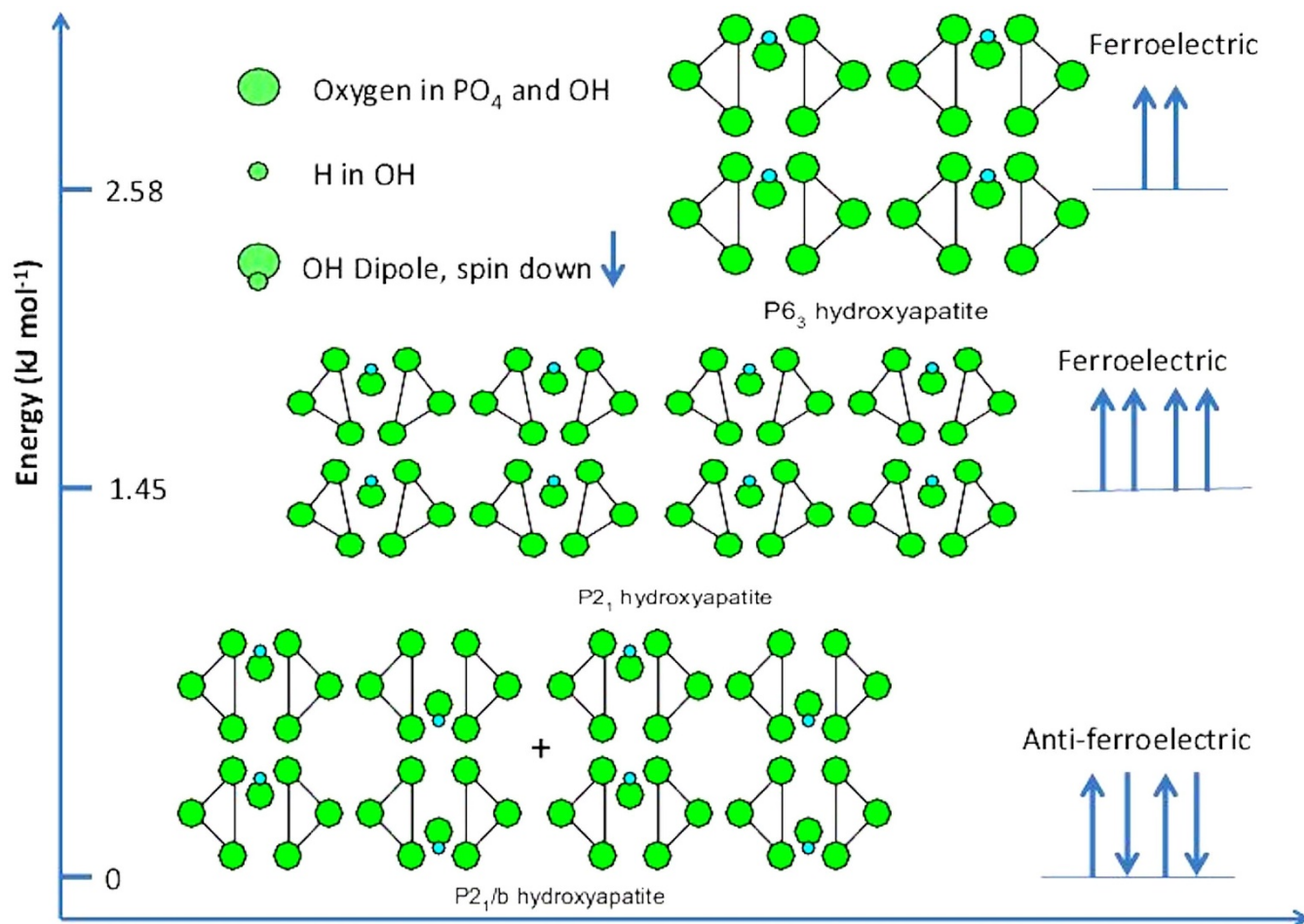


Figure 1 | A schematic representation of the hydroxyl ion orientation and energetics of the nonpolar ($P2_1/b$) and polar symmetries ($P2_1$ and $P6_3$) of hydroxyapatite. The energy cost for a transformation from an antiferroelectric order in hydroxyapatite ion to a ferroelectric order is small.

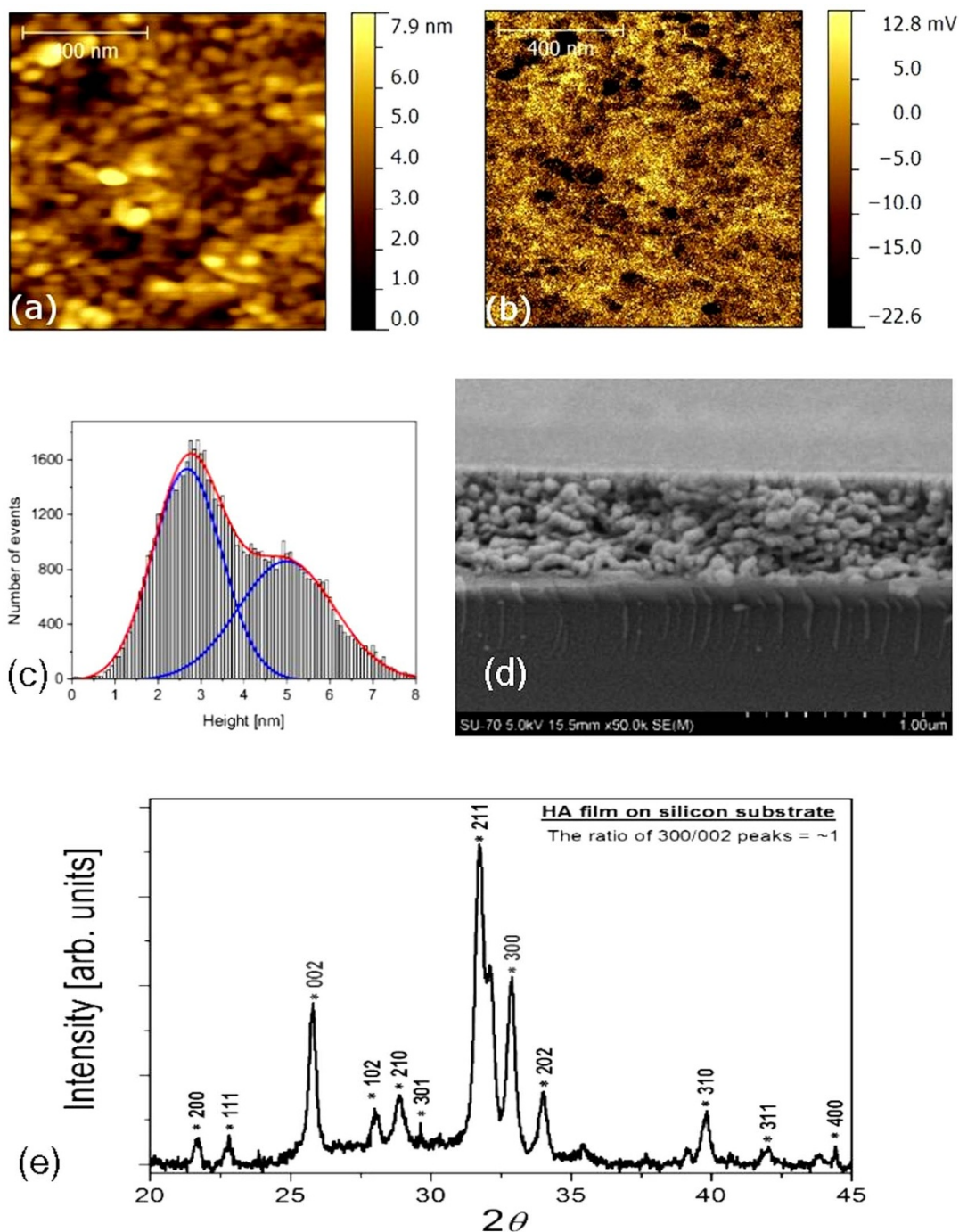


Figure 2 | Representative images of AFM topography (a) and PFM (b) measurements on nanocrystalline hydroxyapatite sample. There is a bimodal distribution in the height variations within the nanocrystals as obtained from AFM topography (c). The shape of the grains varies and ranges from spherical to significantly aspherical grain shape (d). Macroscopically the nanocrystalline film is random but with a slight tendency of orientation towards the crystallographic *c*-axis (e).

Figure 2a and 2b show representative topography measurements and PFM image on nanocrystalline hydroxyapatite films on Si. The topography histograms (Figure 2c) typically exhibit two peaks that represent two types of grains with different growth rates and different properties. High resolution scanning electron micrographs of these films in cross-section show that there are both near-spherical and aspherical grains (Figure 2d). Macroscopically, the film did not possess any uniaxial texture (Figure 2e) but there is a stronger tendency of an orientation towards the crystallographic *c* axis (the ratio of 300/002 peaks ~ 1) than in an otherwise completely random orientation (the ratio of 300/002 peaks ~ 1.8).

Spectroscopic PFM measurements shows the linearity of the measured displacement with the applied ac-voltage (Figure 3) and confirmed the piezoelectric nature of the signal. The slope of the straight line fit gave the value of the effective piezoelectric coefficient which strongly depended on the measurement location.

For hysteresis loop measurements, voltage pulses (U_{dc}) of variable height (up to 100 V) were applied at two different locations on the hydroxyapatite surface indicated on the PFM response images by arrows (Figure 4(a)). The amplitude of the piezoresponse (proportional to d_{33eff}) and phase (which sign indicates polarization direction) were measured immediately after the application of each

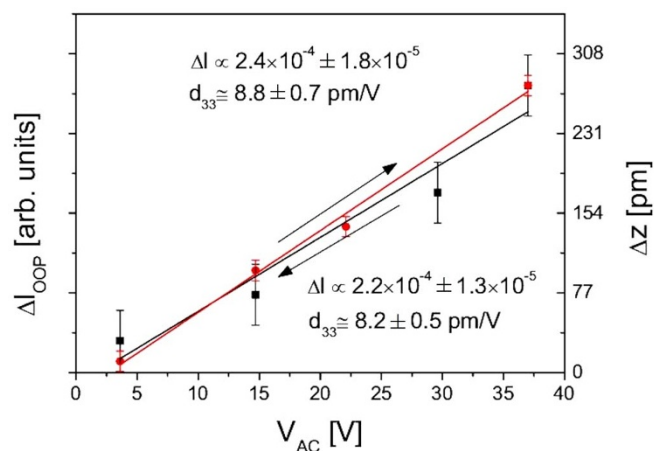


Figure 3 | AC voltage dependence of out-of-plane displacements Δl and Δz for hydroxyapatite film.

poling pulse. The dependencies of both $d_{33\text{eff}}$ and phase with respect to U_{dc} (Figure 4(b)) show a strongly hysteretic dependence typical for polarization switching in ferroelectrics.

In order to demonstrate the stability of the induced polarization (the hysteresis could be purely dynamic as in relaxor ferroelectrics²⁹), we applied a high dc bias to the place where only a grey contrast was observed and measured the piezoresponse after that (Figure 5). The observed behavior suggests that the hydroxyapatite surface indeed becomes polarized and this effect is stable for at least several hours.

Figure 6 shows the ferroelectricity loop measurements on a macroscopic scale by conventional Sawyer-Tower method. There is a

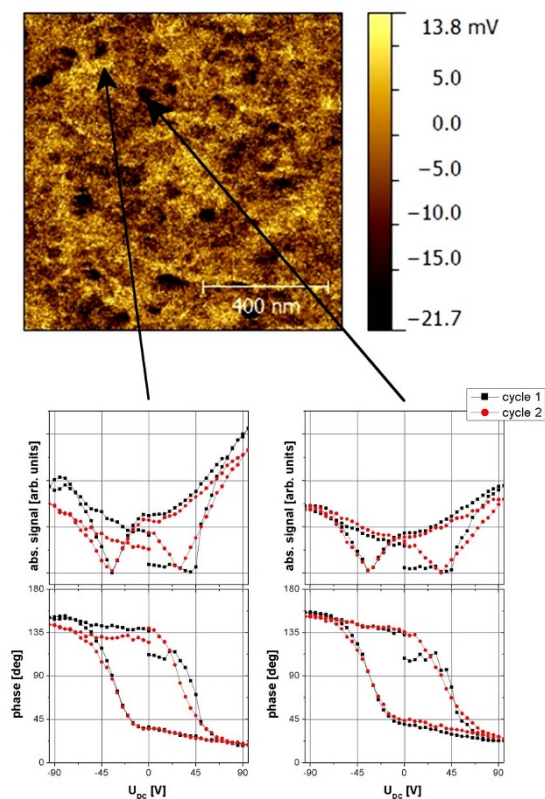


Figure 4 | Representative PFM image (upper part) and recorded ferroelectric hysteresis loops (lower parts) in places indicated by arrows.

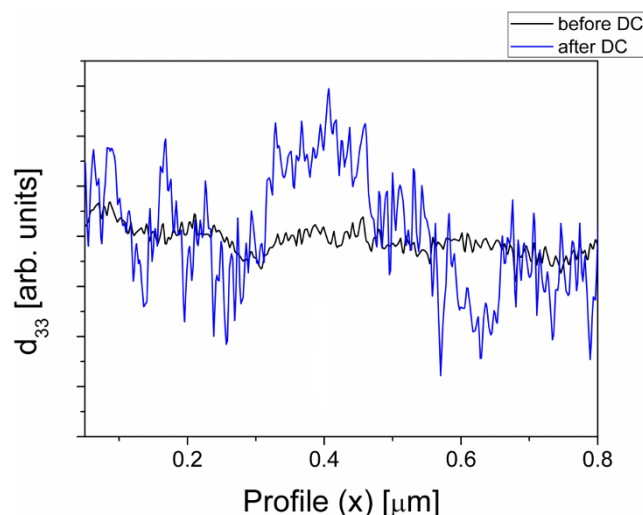


Figure 5 | A cross-section of the piezoelectric response before (black line) and after (blue line) the application of a DC voltage pulse. Polarisation induced in this way was stable for several hours.

hint of polarisation reversal of ferroelectric nature, which has been overshadowed by the strong presence of the leakage current.

Discussion

The topography (Figure 2a) is similar to previous atomic force microscopy images reported in Plecenik et al.²⁸ for solgel deposited thin film hydroxyapatite on Si. The film of hydroxyapatite is built of grains with an average size of about 63 nm and the average root mean square (rms) roughness is about 4 nm. The grain morphology is apparently reflected in the piezoresponse image (Figure 2b), with some correlation between the height of the grain and the amplitude of piezoresponse thus indicating that the observed piezoresponse seems to originate from elevated nanograins. However, there is no one-to-one correspondence between the topography and piezoresponse, so that we can conclude that the spurious effects such as Maxwell force or tip buckling are minimal. The strongest signal corresponds to the effective longitudinal piezoelectric coefficient ($d_{33\text{eff}}$) of about 8 pm/V and varies significantly from grain to grain.

The recorded hysteretic loops are, generally speaking, symmetric. One may observe only a slight shift towards positive values of $d_{33\text{eff}}$ in

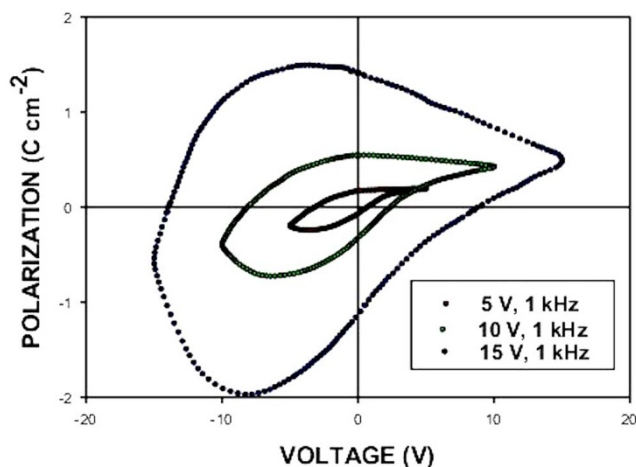


Figure 6 | Conventional Sawyer-Tower macroscopic measurements of ferroelectricity in nanocrystalline HA show that there is a strong contribution from leakage current in P-E measurements.



both cases. It is worth of note that in the case of the loop registered in the “dark” place (the upper part of Figure 4) the coercive field and the remnant $d_{33\text{eff}}$ values are a bit higher than in the loop recorded in the less negative polarized grain. However, this difference is of the order of 10%.

It is to be mentioned that the remnant polarisation in hydroxyapatite film is c.a. 25% of a PZT film measured under the same experimental conditions. The average coercive voltage was found to be around 48 V for both loops. We observed that the phase of piezo-response signal demonstrates continuous variations rather than an abrupt switching behavior characteristic of typical ferroelectrics. It may be related to high piezoelectric losses and can be attributed to the fact that hydroxyapatite is a proton conducting material and high Joule heating may occur under the high voltage applied to the tip.

The most important information which may be concluded from these measurements seems to be the fact of the switching of the hydroxyapatite film by high enough external electric field. It suggests also intrinsically polar character of this material and appearance of piezoelectricity only in some grains when others represent only weak (but still switchable) piezoelectric contrast.

While the local measurements by PFM showed clearly the ferroelectric nature of hydroxyapatite, macroscopic measurements have been less conclusive due to a significant contribution of leakage currents. For example, conventional polarization (P) vs. applied electric field (E) measurements using an automated Sawyer-Tower circuit showed a ferroelectric nature notwithstanding that the contribution of leakage current is significant (Figure 6). Leakage current is a common phenomenon in thin film capacitors. Real ferroelectric capacitors show a leakage current that is superimposed on the displacement current. This can affect the shape of the hysteresis curve³⁰. An integration of the monitored current may then result in a non-physical increase of remnant polarization and coercive field. In the case of hydroxyapatite, the remnant polarization at the macroscopic scale is quite high indicating the presence of the leakage current.

A significant portion of this leakage current originated from the manner the film was electroded using gold electrodes for a ferroelectricity test. The bottom electrode (on Si) was much larger than the top electrode (on the film). This is a standard electrode configuration for microelectronic device testing. Because the “bottom” electrode was much larger than the top electrode, the sample with such configuration could still be regarded as a single parallel capacitor of which the electrode area was equal to the area of the “top” electrode and the thickness was equal to the thickness of the ferroelectric film. The problem that the sample was still leaky was simply because the top electrode was still too large. Photolithographic electroding could have reduced the electrode size and hence reduced the leakage current. This was avoided due to the fear of chemical change of the film. Ferroelectric PZT films tested in a similar way also exhibited similar leaky behavior simply because the electrode size was large. This is why we only extracted physical parameters such as coercive field and remnant polarization from macroscopic measurements, although the ferroelectric nature of the film could be qualitatively observed.

The most important information which may be concluded from these measurements is the switching of the hydroxyapatite film by the external electric field. It proves the polar character of this material. Aortic ferroelectricity has been directly linked with negative consequences such as the initial stages of atherosclerosis, as well as for the gradual destruction and impairment of the arterial wall (aneurysm)⁷. While piezoelectric polarization has been generally considered to be linked with positive consequences in the cell-mediated bone growth³¹, our report on ferroelectricity in hydroxyapatite will generate investigations on ferroelectricity in hard tissues, its physiological implications. Ferroelectricity in hydroxyapatite films means that it can be easily polarised/depolarised by using an external electrical field. This can be effectively used in understanding the role of

surface charge and interfacial charge in mediating biological reactions on biomaterials surface³².

Nanoscale dimensions and an orderly assemblage of inorganic crystals have been reported to be responsible for ferroelectric-like hysteresis loops in bio-assembled, hierarchical architectures of nano-CaCO₃ laminas sandwiched between biopolymers in conch shells³³. The effect is however more of a ferroelectret nature, where ferroelectric-like hysteresis originate from the materials charge storing capability (electret is a term coined in analogy to ‘magnet’ for magnetic polarisation). The role of aragonite, which is known as a centrosymmetric crystal devoid of piezo, pyro and ferroelectricity, is also not very clear. In contrast, nanocrystalline hydroxyapatite shows strong piezo, pyro and ferroelectric behaviour of classical nature and opens up potential for its applications in bio-energy harvesting, biosensing and even in biocompatible electronics and MEMS devices.

Methods

Thin films of hydroxyapatite has been prepared by using a sol-gel method followed by spin coating on (100) Si. Phosphorus pentoxide (P₂O₅) and calcium nitrate tetrahydrate (Ca(NO₃)₂ · (H₂O)₄) were dissolved in absolute ethanol. These two solutions were combined slowly in a Ca/P molar ratio of 1.67. The mixture was continuously stirred and heated at 60°C for 1 h. The resulting sol was spin-coated on the (100) surfaces of n-doped silicon wafers. The wafers were dried for 1–2 h at 200°C, then calcined at 700°C for 1 h with heating and cooling rates of 5°C min⁻¹. The hydroxyapatite film thickness has been determined by a field-emission gun scanning electron microscope (FEG-SEM, Model: Joel JSM-840). The micrograph (Figure 2d) shows the cross section of the hydroxyapatite on silicon. The thickness of the film is about 500 nm. The phase identification of the film has been examined by glancing angle X-ray diffraction (XRD, Philips X’Pert PRO MPD) using a graphite-monochromatized Cu-K α radiation at 40 kV and 35 mA. X-ray diffraction was used to investigate crystalline structure of the film. The XRD pattern (Figure 2e) shows characteristic peaks of hydroxyapatite, matched with the standard hydroxyapatite peaks (JCPDS 9-432), and reveals that the film is nanocrystalline with broad peaks but phase-pure with no common thermally decomposed phases of hydroxyapatite such as CaO or tricalcium phosphate (TCP). The chemistry of the surface was established by the use of a Kratos Axis 165 Spectrometer and a Perkin Elmer Fourier Transform Infra Red Spectroscopy. PFM measurements were done with a commercial AFM (Multimode SPM, Bruker) equipped with external function generator and lock-in amplifier. We used doped Si cantilevers with spring constants in the range of 1.2–29 N/m driven at a frequency of 10 kHz. Macroscopic ferroelectricity measurements were made by using conventional Sawyer-Tower P-E loop plotter. The sample was tested by using gold electrodes. A “dot”-like gold electrode (diameter of ~200 μ m) was sputter deposited on the HA film as the top electrode and a very large area (> mm² in area) was sputter deposited on the Si substrate as the bottom electrode. The size of the electrodes was defined by using shadow masks.

1. Bocchi, G. & Valdre, G. Physical, chemical, and mineralogical characterization carbonate-hydroxyapatite concretions of the human pineal gland. *J. Inorgan. Biochem.* **49**, 209–220 (1993).
2. Calvert, P. & Mann, S. The negative side of crystal growth. *Nature* **386**, 127–129 (1997).
3. Yamashita, S., Oikawa, N. & Umegaki, T. Acceleration and deceleration of bone-like crystal growth on ceramic hydroxyapatite by electric poling. *Chemical Materials* **8**, 2697–2700 (1996).
4. Nakamura, S., Kobayashi, T. & Kimihiro, Y. Numerical osteobonding evaluation of electrically polarized hydroxyapatite ceramics. *Journal of Biomedical Materials Research A* **68A**, 90–94 (2004).
5. Sawyer, P. N. & Harshaw, D. H. *Biophys. J.* **6**, 663 (1966).
6. Horiuchi, S. *et al.* Above-room-temperature ferroelectricity and antiferroelectricity in benzimidazoles. *Nature Communications* **3**, 1308 (2012).
7. Boldrini, P. Ferroelectricity in the Arterial Wall: A New Physical Component of Atherosclerosis. *Journal of Theoretical Biology* **87**, 263–273 (1980).
8. Liu, Y., Zhang, Y., Chow, M.-J., Chen, Q. N. & Li, J. Biological ferroelectricity uncovered in aortic walls by piezoresponse force microscopy. *Phys. Rev. Lett.* **108**, 78103 (2012).
9. Martin, R. B. Anomalous Piezoelectric Behaviour in Dry Bone. in *Electrical Properties of Bone and Cartilage: Experimental Effects and Clinical Applications* (eds Brighton, C. T., Black, C. T. & Pollack, S. R.) 31–45 (Grune and Straton, 1979).
10. Denning, D., Alilat, S., Habelitz, S., Fertala, A. & Rodriguez, B. J. Visualizing molecular polar order in tissues via electromechanical coupling. *Journal of Structural Biology* **180**, 409–419 (2012).
11. Chiatti, F., Corno, M. & Ugliengo, P. Stability of the dipolar (001) surface of hydroxyapatite. *Journal of Physical Chemistry C* **116**, 6108–6114 (2012).
12. Fukada, E. & Yasuda, I. On the piezoelectric effect of bone. *J. Phys. Soc. Jpn.* **12**, 1158–1162 (1957).



13. Lang, S. B. Pyroelectric effect in bone and tendon. *Nature* **212**, 704–705 (1966).
14. Kay, M. I., Young, R. A. & Posner, A. S. Crystal structure of hydroxyapatite. *Nature* **204**, 1050 (1964).
15. Haverty, D., Tofail, S. A. M., Stanton, K. T. & McMonagle, J. B. Structure and stability of hydroxyapatite: Density functional calculation and Rietveld analysis. *Phys. Rev. B* **71**, 94103 (2005).
16. Tofail, S. A. M., Haverty, D., Stanton, K. T. & McMonagle, J. B. Structural order and dielectric behaviour of hydroxyapatite. *Ferroelectrics* **319**, 117–123 (2005).
17. Amis, E. J. & Rumble, J. Certificate of analysis, SRM 2910: Calcium hydroxyapatite. (2003).
18. Tofail, S. A. M., Baldisserrri, C., Haverty, D., McMonagle, J. B. & Erhart, J. Pyroelectric surface in hydroxyapatite ceramics. *J. Appl. Phys.* **106**, 106104 (2009).
19. Tofail, S. A. M. *et al.* Direct and ultrasonic measurements of macroscopic piezoelectricity in sintered hydroxyapatite. *J. Appl. Phys.* **105**, 64103 (2009).
20. Lang, S. B. *et al.* Pyroelectric, piezoelectric and photoeffects in hydroxyapatite thin films on silicon. *App. Phys. Lett.* **98**, 123703 (2011).
21. Xu, Y. *Ferroelectric Materials and Their Applications*. **330**, (North-Holland 1991).
22. Bukowski, T. J. *et al.* Piezoelectric Properties of Sol-Gel Derived ZnO Thin Films. *Integrated Ferroelectrics* **17**, 339–347 (1997).
23. Kalinin, S. V., Setter, N. & Kholkin, A. Electromechanics on the nanometer scale: emerging phenomena, devices, and applications. *MRS Bull.* **34**, 634 (2009).
24. Gruverman, A., Auciello, O. & Tokumoto, H. Scanning force microscopy: application to nanoscale studies of ferroelectric domains. *Integr. Ferroelectr.* **19**, 49–83 (1998).
25. Bdikin, I. D. *et al.* Polarization switching and patterning in self-assembled peptide tubular structures. *J. Appl. Phys.* **111**, 74104 (2012).
26. Kholkin, A., Amdursky, N., Bdikin, I. D., Gazit, E. & Rosenman, G. Strong piezoelectricity in bioinspired peptide nanotubes. *ACS Nano* **4**, 610–614 (2010).
27. Heredia, A. *et al.* Nanoscale ferroelectricity in crystalline γ -glycine. *Adv. Funct. Mater.* **22**, 2996–3003 (2012).
28. Plecenik, T. *et al.* *Journal of Materials Science: Materials for Medicine* **23**, 47–50 (2012).
29. Kholkin, A. *et al.* Surface-induced domain structures and mesoscopic phase transition in relaxor ferroelectrics. *Advances in Functional Materials* **21**, 1977 (2011).
30. Lee, H. N., Hesse, D., Zahkharov, N. & Gosele, U. Ferroelectric Bi_{3.25}La_{0.75}Ti₃O₁₂ films of uniform a-axis orientation on silicon substrates. *Science* **296**, 2006 (2002).
31. Inoue, S. *Electric stimulation of osteogenesis in the rat: Amperage of three different stimulation methods.* in *Electrical Properties of Bone and Cartilage: Experimental Effects and Clinical Applications* (eds Brighton, C. T., Black, J. & Pollack, S. R.) 199–213 (Grune and Straton, 1979).
32. Robin, S. *et al.* Charge specific protein placement at submicrometer and nanometer scale by direct modification of surface potential by electron beam. *Langmuir* **27**, 14968–14974 (2011).
33. Yao, Y. *et al.* Bio-Assembled Nanocomposites in Conch Shells Exhibit Giant Electret Hysteresis. *Advanced Materials* **25**, 711–718 (2013).

Acknowledgements

This project has been funded with support from the European Commission _Grant No. EC NMP4-SL-2008-CP-212533-2—BioElectricSurface. This publication reflects the views only of the authors, and the Commission cannot be held responsible for any use which may be made of the information contained therein. MW acknowledges the support of a research fellowship from the Polish Ministry of Science and Higher Education, grant No. 657/MOB/2011/0. The Field Emission SEM was funded by the Higher Education Authority (HEA) under the PRTL4 program within the INSPIRE consortium. SB and MK gratefully acknowledge financial support from the European Research Council within the Advanced Investigators Grant “Soft-Map”.

Author contributions

The materials were prepared by M.G., S.A.M.T., A.A.G. and A.P. Experimental measurements and associated figures (Figures 2–6) were made by S.B.L., S.A.M.T., A.L.K., M.W., A.A.G., Y.W., S.B. and M.K. Figure 1 was prepared by S.A.M.T. The manuscript was written by S.B.L., S.A.M.T. and A.L.K. All authors reviewed the manuscript.

Additional information

Competing financial interests: The authors declare no competing financial interests.

How to cite this article: Lang, S.B. *et al.* Ferroelectric Polarization in Nanocrystalline Hydroxyapatite Thin Films on Silicon. *Sci. Rep.* **3**, 2215; DOI:10.1038/srep02215 (2013).



This work is licensed under a Creative Commons Attribution-NonCommercial-NoDerivs 3.0 Unported license. To view a copy of this license, visit <http://creativecommons.org/licenses/by-nc-nd/3.0>